

$np \rightarrow d\gamma$  for Big-Bang NucleosynthesisJiunn-Wei Chen<sup>a</sup>, and Martin J. Savage<sup>a,b</sup><sup>a</sup> *Department of Physics, University of Washington,  
Seattle, WA 98195.*<sup>b</sup> *Jefferson Lab., 12000 Jefferson Avenue, Newport News,  
Virginia 23606.*

## Abstract

The cross section for  $np \rightarrow d\gamma$  is calculated at energies relevant to big-bang nucleosynthesis using the recently developed effective field theory that describes the two-nucleon sector. The E1 amplitude is computed up to N<sup>3</sup>LO and depends only upon nucleon-nucleon phase shift data. In contrast, the M1 contribution is computed up to NLO, and the four-nucleon-one-magnetic-photon counterterm that enters is determined by the cross section for cold neutron capture. The uncertainty in the calculation for nucleon energies up to  $E \sim 1$  MeV is estimated to be  $\lesssim 4\%$ .

July, 1999

The radiative capture process  $np \rightarrow d\gamma$  is a key reaction in the synthesis of nuclei in the early universe. Recently, it has been emphasized by Burles, Nollet, Truran and Turner (BNTT) [1] that the uncertainty in the cross section [2] of  $np \rightarrow d\gamma$  at energies relevant for big-bang nucleosynthesis (BBN) is difficult to determine due to the lack of data at low energies and the lack of information about theoretical estimates. In determining theoretical uncertainties in the abundances of the elements produced in BBN, Smith, Kawano and Malaney (SKM) [3] assigned a  $1\sigma$  error of 5% to the cross section for  $np \rightarrow d\gamma$ , which was also used in the recent analysis of BNTT [1]. In [1] it was found that this 5% uncertainty contributes a significant fraction of the uncertainties in the abundances of elements produced in BBN.

In this work we compute the cross section of  $np \rightarrow d\gamma$  using the recently developed techniques of effective field theory in the two-nucleon sector [4,5]. For the energy range appropriate for BBN (nucleon energies  $E_N \lesssim 1\text{MeV}$ ) it is appropriate to use the effective field theory of only nucleons and photons, as presented in [6], which we denote by EFT( $\not{\pi}$ ). The cross section of  $np \rightarrow d\gamma$  for cold neutrons has been computed in the theory with pions [7] and in EFT( $\not{\pi}$ ) [6] up to next-to-leading order (NLO) in the effective field theory expansion parameter(s). For cold neutrons the cross section is dominated by M1-capture from the  $^1S_0$  channel via the nucleon isovector magnetic moment. However, in addition to the contribution from the effective ranges of both the  $^1S_0$  and  $^3S_1$  channels at NLO, there is a contribution from a four-nucleon-one-magnetic-photon interaction with a coefficient,  $^{\not{\pi}}L_1^{(M1)}$ , that is not constrained by nucleon-nucleon scattering phase shift data. The observed cross section for cold neutrons determines  $^{\not{\pi}}L_1^{(M1)}$ . At higher energies,  $E_N \sim 1\text{ MeV}$ , the cross section for  $np \rightarrow d\gamma$  is dominated by the E1-capture of nucleons in a relative P-wave,  $^3P_0$ ,  $^3P_1$ , and  $^3P_2$ . In the energy region relevant to BBN the contributions from both E1- and M1-capture are important.

It is important to emphasize that the results of our calculation look very similar to those of effective range theory (ER) [8,9] (for a detailed discussion see [10]). One of the interesting results from the recent developments in effective field theory is that ER is seen to reproduce the leading orders of any particular amplitude for low energy processes. However, ER fails to reproduce the true amplitude at and beyond the order at which there is a contribution from a local, multi-nucleon-external-field interaction [6]. If multi-nucleon-external-field interactions do not enter until very high orders in the EFT( $\not{\pi}$ ) expansion, then ER will reproduce the observed value to high precision, as is the case for the polarizability of the deuteron [6,11]. However, if a multi-nucleon-external-field interaction occurs at low orders ER can deviate substantially from the true result, as is the case for the capture of cold neutrons,  $np \rightarrow d\gamma$  [7], or the deuteron quadrupole moment [5]. For this process, the conventional understanding of this discrepancy is that important contributions from meson-exchange currents have been omitted [12]. However, in effective field theory, this discrepancy results from the omission of four-nucleon-one-magnetic-photon operators that enter at NLO and higher in the expansion. For  $np \rightarrow d\gamma$  at finite but low incident nucleon energy, the two dominant amplitudes, E1 and M1, behave differently in the effective field theory expansion. In EFT( $\not{\pi}$ ), a four-nucleon-one-electric-dipole-photon local operator occurs at N<sup>4</sup>LO, which means that the E1 amplitude can be computed up to N<sup>3</sup>LO with knowledge of only the nucleon-nucleon scattering phase shifts. Therefore, this amplitude will look very similar to the expression obtained in ER, when a  $\gamma\rho$  expansion is performed. In contrast, the M1 amplitude receives

a contribution from a four-nucleon-one-magnetic-photon at NLO, and therefore the effective field theory result will deviate from that obtained in ER in a significant way. In addition to the expressions we obtain for both the E1 and M1 amplitudes being analytic and compact, they are perturbatively close to the true amplitudes for this process, giving a total cross section that deviates  $\lesssim 4\%$  over the range of center-of-mass kinetic energies below 1 MeV. In our calculation we neglect both isospin violation and relativistic effects, as in the energy region of interest both effects are significantly smaller than the uncertainty introduced by not computing beyond the order to which we work (relativistic effects are formally NNLO in EFT( $\not\tau$ ) [6], but are suppressed by additional factors of  $m_\pi^2/M_N^2$  compared to other NNLO effects).

The strong interactions between two nucleons in the  ${}^3S_1$ -channel are determined by the lagrange density, up to N<sup>3</sup>LO,

$$\begin{aligned} \mathcal{L}_2^{(3S_1)} = & -\not\tau C_0^{(3S_1)} (N^T P_i N)^\dagger (N^T P_i N) + \frac{1}{8} \not\tau C_2^{(3S_1)} \left[ (N^T P_i N)^\dagger (N^T \mathcal{O}_i^{(2)} N) + h.c. \right] \\ & - \frac{1}{16} \not\tau C_4^{(3S_1)} (N^T \mathcal{O}_i^{(2)} N)^\dagger (N^T \mathcal{O}_i^{(2)} N) - \frac{1}{32} \not\tau \tilde{C}_4^{(3S_1)} \left[ (N^T \mathcal{O}_i^{(4)} N)^\dagger (N^T P_i N) + h.c. \right] \\ & + \frac{1}{128} \not\tau C_6^{(3S_1)} \left[ (N^T \mathcal{O}_i^{(4)} N)^\dagger (N^T \mathcal{O}_i^{(2)} N) + h.c. \right] \end{aligned} \quad (1)$$

where  $P_i$  is the spin-isospin projector for the  ${}^3S_1$  channel

$$P_i \equiv \frac{1}{\sqrt{8}} \sigma_2 \sigma_i \tau_2 \quad , \quad \text{Tr } P_i^\dagger P_j = \frac{1}{2} \delta_{ij} \quad . \quad (2)$$

The Galilean invariant derivative operators  $\mathcal{O}^{(2)}$  and  $\mathcal{O}^{(4)}$  are defined by

$$\begin{aligned} \mathcal{O}_i^{(2)} &= P_i \overleftrightarrow{\mathbf{D}}^2 + \overleftarrow{\mathbf{D}}^2 P_i - 2 \overleftarrow{\mathbf{D}} P_i \overrightarrow{\mathbf{D}} \\ \mathcal{O}_i^{(4)} &= P_i \overleftrightarrow{\mathbf{D}}^4 - 4 \overleftarrow{\mathbf{D}} P_i \overrightarrow{\mathbf{D}}^3 + 6 \overleftarrow{\mathbf{D}}^2 P_i \overrightarrow{\mathbf{D}}^2 - 4 \overleftarrow{\mathbf{D}}^3 P_i \overrightarrow{\mathbf{D}} + \overleftarrow{\mathbf{D}}^4 P_i \quad , \end{aligned} \quad (3)$$

where the covariant derivative is defined to be  $\mathbf{D} = \nabla - ieQ\mathbf{A}$ . The superscript on the coefficient denotes the number of derivatives in the operator. The expansion parameters of EFT( $\not\tau$ ) are the external momentum involved in the particular process normalized to the mass of the pion,  $Q \sim p/m_\pi$ . For momenta of order the pion mass or greater this expansion will fail to converge. We have not shown the other operator involving six derivatives as it does not contribute to  $np \rightarrow d\gamma$  at the order to which we are working. In order that the deuteron pole is not shifted order-by-order in the  $Q$ -expansion, the coefficients appearing in eq. (1) have expansions in powers in  $Q$ , e.g.

$$\not\tau C_0^{(3S_1)} = \not\tau C_{0,-1}^{(3S_1)} + \not\tau C_{0,0}^{(3S_1)} + \not\tau C_{0,1}^{(3S_1)} + \dots \quad . \quad (4)$$

The second subscript on each coefficient denotes the powers of  $Q$  in the coefficient itself. Relating the S-matrix obtained from the lagrange density in eq. (1) to that described by the effective range expansion,

$$|\mathbf{k}| \cot \delta_0 = -\gamma_t + \frac{1}{2} \rho_d (|\mathbf{k}|^2 + \gamma_t^2) + w_2 (|\mathbf{k}|^2 + \gamma_t^2)^2 + \dots \quad , \quad (5)$$

one can fix most of the coefficients (only one linear combination of  $\not{C}_4^{(3S_1)}$  and  $\not{C}_4^{(3S_1)}$  contributes to NN scattering) appearing in eq. (1) in terms of  $\gamma_t^{-1} = 4.318946$  fm ( $\gamma_t$  is the deuteron binding momentum),  $\rho_d = 1.764 \pm 0.002$  fm (the effective range parameter), and  $w_2 = 0.389$  fm<sup>3</sup> (the shape parameter) [13]. The neglect of relativistic effects allows us to set  $\gamma_t = \gamma = \sqrt{M_N B}$  where  $B = 2.224575$  MeV is the deuteron binding energy. In addition, to the order we are working mixing between the  ${}^3S_1$  and  ${}^3D_1$  channels does not contribute, and so we will not discuss this sector. However, there is a contribution from P-wave final state interactions in the E1-capture process that enter at N<sup>3</sup>LO. The P-wave interactions are described at leading order by the lagrange density

$$\begin{aligned} \mathcal{L}_2^P = & \left( \not{C}_2^{(3P_0)} \delta^{xy} \delta^{wz} + \not{C}_2^{(3P_1)} [\delta^{xw} \delta^{yz} - \delta^{xz} \delta^{yw}] + \not{C}_2^{(3P_2)} \left[ 2\delta^{xw} \delta^{yz} + 2\delta^{xz} \delta^{yw} - \frac{4}{3} \delta^{xy} \delta^{wz} \right] \right) \\ & \times \frac{1}{4} \left( N^T \mathcal{O}_{xy}^{(1,P)} N \right)^\dagger \left( N^T \mathcal{O}_{wz}^{(1,P)} N \right) \quad , \end{aligned} \quad (6)$$

where the P-wave operators are

$$\mathcal{O}_{ij}^{(1,P)} = \overleftarrow{\mathbf{D}}_i P_j^{(P)} - P_j^{(P)} \overrightarrow{\mathbf{D}}_i \quad , \quad (7)$$

and  $P_i^{(P)}$  is the spin-isospin projector for the isotriplet, spintriplet channel

$$P_i^{(P)} \equiv \frac{1}{\sqrt{8}} \sigma_2 \sigma_i \tau_2 \tau_3 \quad , \quad \text{Tr } P_i^{(P)\dagger} P_j^{(P)} = \frac{1}{2} \delta_{ij} \quad . \quad (8)$$

The measured P-wave phase shifts (as given by the Nijmegen phase shift analysis [14]) fix the coefficients appearing in eq. (6) to be

$$\not{C}_2^{(3P_0)} = +6.53 \text{ fm}^4 \quad , \quad \not{C}_2^{(3P_1)} = -5.91 \text{ fm}^4 \quad \text{and} \quad \not{C}_2^{(3P_2)} = +0.57 \text{ fm}^4 \quad . \quad (9)$$

Finally, there are interactions with the electromagnetic field that are not simply related by gauge invariance to the strong interaction dynamics. The lagrange density describing the leading interactions that contribute to  $np \rightarrow d\gamma$  is

$$\begin{aligned} \mathcal{L}_{2,B} = & \left[ e \not{L}_1^{(M1)} (N^T P_i N)^\dagger (N^T \overline{P}_3 N) \mathbf{B}_i + \text{h.c.} \right. \\ & + \frac{1}{2} e \not{L}_1^{(E1)} (N^T \mathcal{O}_{ia}^{(1,P)} N)^\dagger (N^T P_a N) \mathbf{E}_i + \text{h.c.} \\ & \left. - \frac{1}{8} e \not{L}_3^{(E1)} (N^T \mathcal{O}_{ia}^{(1,P)} N)^\dagger (N^T \mathcal{O}_a^{(2)} N) \mathbf{E}_i + \text{h.c.} \right] \quad , \end{aligned} \quad (10)$$

where  $\mathbf{E}$  is the electric field,  $\mathbf{B} = \nabla \times \mathbf{A}$  is the magnetic field, and where

$$\overline{P}_3 = \frac{1}{\sqrt{8}} \sigma_2 \tau_2 \tau_3 \quad , \quad (11)$$

is the projector for the  ${}^1S_0$  channel. The renormalization group (RG) evolution of  $\not{L}_1^{(M1)}$  has been discussed in [7], and the evolution of the electric coefficients are determined by

$$\mu \frac{d}{d\mu} \left[ \frac{\not{L}_1^{(E1)} - M_N \not{C}_{4,-2}^{(3S_1)}}{\not{C}_{0,-1}^{(3S_1)}} \right] = 0 \quad , \quad \mu \frac{d}{d\mu} \left[ \frac{\not{L}_3^{(E1)} - M_N \not{C}_{6,-4}^{(3S_1)}}{\not{C}_{0,-1}^{(3S_1)}} \right] = 0 \quad . \quad (12)$$

These RG equations tell us (by considering the size of the quantities in square brackets at  $\mu = m_\pi$ , the matching scale) that the combination  $\not{L}_1^{(E1)} - M_N \not{C}_{4,-2}^{(3S_1)}$  is of order  $Q^{-1}$  or higher, as opposed to the naive counting of  $Q^{-2}$  and that  $\not{L}_3^{(E1)} - M_N \not{C}_{6,-4}^{(3S_1)}$  is of order  $Q^{-1}$  or higher, as opposed to  $Q^{-4}$ .

The amplitude for  $np \rightarrow d\gamma$  can be written as

$$T = e X_{E1} U_n^T \tau_2 \tau_3 \sigma_2 \sigma \cdot \epsilon_{(d)}^* U_p \mathbf{P} \cdot \epsilon_{(\gamma)}^* + ie X_{M1} \varepsilon^{abc} \epsilon_{(d)}^{*a} \mathbf{k}^b \epsilon_{(\gamma)}^{*c} U_n^T \tau_2 \tau_3 \sigma_2 U_p \quad , \quad (13)$$

where we have not shown amplitudes that contribute much less than 1% to the total capture cross section in the energy range of interest, leaving only the isovector E1 and the isovector M1 amplitudes.  $U_n$  is the neutron two-component spinor and  $U_p$  is the proton two-component spinor.  $|\mathbf{P}|$  is the magnitude of the momentum of each nucleon in the center of mass frame, while  $\mathbf{k}$  is the photon momentum. The photon polarization vector is  $\epsilon_{(\gamma)}$ , and  $\epsilon_{(d)}$  is the deuteron polarization vector. For convenience, we define dimensionless variables  $\tilde{X}$ , by

$$\frac{|\mathbf{P}| M_N}{\gamma^2} X_{E1} = i \frac{2}{M_N} \sqrt{\frac{\pi}{\gamma^3}} \tilde{X}_{E1} \quad , \quad X_{M1} = i \frac{2}{M_N} \sqrt{\frac{\pi}{\gamma^3}} \tilde{X}_{M1} \quad , \quad (14)$$

In terms of these amplitudes, the total cross section for  $np \rightarrow d\gamma$  is

$$\sigma = \frac{4\pi\alpha (\gamma^2 + |\mathbf{P}|^2)^3}{\gamma^3 M_N^4 |\mathbf{P}|} \left[ |\tilde{X}_{M1}|^2 + |\tilde{X}_{E1}|^2 \right] \quad , \quad (15)$$

where we have used nonrelativistic kinematics, as is appropriate for the energy region of interest.

Explicit calculation of  $|\tilde{X}_{E1}|^2$  up to N<sup>3</sup>LO (i.e.  $Q^1$ ) gives

$$|\tilde{X}_{E1}|^2 = \frac{|\mathbf{P}|^2 M_N^2 \gamma^4}{(\gamma^2 + |\mathbf{P}|^2)^4} \left[ 1 + \gamma\rho_d + (\gamma\rho_d)^2 + (\gamma\rho_d)^3 + \frac{M_N \gamma}{6\pi} \left( \frac{\gamma^2}{3} + |\mathbf{P}|^2 \right) \left( \not{C}_2^{(3P_0)} + 2 \not{C}_2^{(3P_1)} + \frac{20}{3} \not{C}_2^{(3P_2)} \right) \right] \quad . \quad (16)$$

The momentum expansion of the theory is made explicit in eq. (16), and it is clear that we have captured all terms up to and including  $(\gamma/m_\pi)^3$ , and  $(|\mathbf{P}|/m_\pi)^3$ . Terms that have been omitted are of the form  $(\gamma\rho_d)^4 \sim 0.03$ ,  $(|\mathbf{P}|\rho_d)^4 \sim 0.006$  and higher and also relativistic corrections of the form  $(\gamma/M_N)^2 \sim 0.002$ , or  $(|\mathbf{P}|/M_N)^2 \sim 0.001$  and higher, for nucleon energies of  $E \sim 1$  MeV. It is interesting to note that contributions from  $\not{C}_4^{(3S_1)}$  and  $\not{C}_6^{(3S_1)}$  occur at N<sup>3</sup>LO. However, there are also contributions from the four-nucleon-one-electric-photon operators in eq. (10) with coefficients that exactly reproduce the renormalization scale independent quantities that occur in eq. (12). Therefore, these combinations are higher order than N<sup>3</sup>LO. The relative contributions from the P-wave final state interactions entering at N<sup>3</sup>LO are much smaller than the  $(\gamma\rho_d)^3$  contribution also entering at N<sup>3</sup>LO.

The M1-capture contribution  $|\tilde{X}_{M1}|^2$  has been computed up to NLO (i.e.  $Q^1$ ) for the capture of cold-neutrons in the theory with pions [7] and EFT( $\not{\pi}$ ) [6]. It is straightforward to extend these results to the capture of nucleons with non-zero momentum, and at NLO we find

$$|\tilde{X}_{M1}|^2 = \frac{\kappa_1^2 \gamma^4 \left(\frac{1}{a_1} - \gamma\right)^2}{\left(\frac{1}{a_1^2} + |\mathbf{P}|^2\right) (\gamma^2 + |\mathbf{P}|^2)^2} \left[ 1 + \gamma \rho_d - r_0 \frac{\left(\frac{\gamma}{a_1} + |\mathbf{P}|^2\right) |\mathbf{P}|^2}{\left(\frac{1}{a_1^2} + |\mathbf{P}|^2\right) \left(\frac{1}{a_1} - \gamma\right)} - \frac{\not{L}_{np} M_N \gamma^2 + |\mathbf{P}|^2}{\kappa_1 2\pi \frac{1}{a_1} - \gamma} \right], \quad (17)$$

where  $\kappa_1$  is the isovector nucleon magnetic moment,  $a_1 = -23.714 \pm 0.013$  fm is the scattering length in the  $^1S_0$  channel and  $r_0 = 2.73 \pm 0.03$  fm is the effective range in the  $^1S_0$  channel. The constant  $\not{L}_{np}$  is a RG invariant combination of parameters,

$$\not{L}_{np} = (\mu - \gamma) \left(\mu - \frac{1}{a_1}\right) \left[ \not{L}_1^{(M1)} - \frac{\pi \kappa_1}{M_N} \left( \frac{r_0^{(^1S_0)}}{\left(\mu - \frac{1}{a^{(^1S_0)}}\right)^2} + \frac{\rho_d}{(\mu - \gamma)^2} \right) \right], \quad (18)$$

that must be determined from data. It is simplest to determine  $\not{L}_{np}$  from the cross section for cold neutron capture, that is dominated by the M1 matrix element. For incident neutrons with speed  $|v| = 2200$  m/s the cross section for capture by protons at rest is measured to be  $\sigma^{\text{expt}} = 334.2 \pm 0.5$  mb [15]. The value of  $\not{L}_{np}$  required to reproduce a cross section of 334.2 mb is  $\not{L}_{np} = -4.513$  fm<sup>2</sup> (the experimental uncertainty in this measurement introduces a negligible uncertainty in our predictions and we have used the isopin averaged value of the nucleon mass,  $M_N = 938.92$ ). The largest uncertainty in the M1 contribution to the total cross section is expected to be of the form  $|\mathbf{P}| \gamma \rho_d^2$ , which is  $\sim 10\%$  at an energy of 1 MeV (corrections of the form  $\gamma^2 \rho_d^2$  have been renormalized away by fitting  $\not{L}_{np}$  to the cold neutron capture cross section). Given that for energies above  $\sim 200$  keV the E1 amplitude dominates the cross section, a relatively large uncertainty in the M1 amplitude does not lead to a large uncertainty in the total cross section. In fact, we find that by assigning an uncertainty of 3% to the E1 cross section and an uncertainty of the form  $|\mathbf{P}| \gamma \rho_d^2$  to the M1 contribution, the uncertainty in the total cross section is  $\lesssim 4\%$  (the maximum uncertainty occurring at an energy of  $\sim 200$  keV), where we have added the errors linearly. For energies below 8 keV the uncertainty drops to below 1%.

At LO, the expression in eq. (17) for the M1 amplitude reproduces the analogous expression found in ER [8,9] (after the typographical errors in [9] have been corrected [6]). However, at NLO where the effective range parameters  $\rho_d$  and  $r_0$  first appear the expression differs both qualitatively and quantitatively. The ER amplitude does not correctly describe physics at distance scales of order  $1/m_\pi$  or shorter. In EFT( $\not{\mathcal{L}}$ ), physics at such distance scales, beyond the physics of NN scattering alone, is reproduced by the local counterterm  $\not{L}_{np}$ .

A comparison between the cross section obtained with effective field theory and the numerical values obtained from the on-line nuclear data center [2] is shown in table I. One sees that the analytic expressions we have obtained reproduces very well (within a few percent) the numerical values of ref. [2]. However, at  $E = 1$  keV the EFT( $\not{\mathcal{L}}$ ) cross section is  $\sim 2.5\%$  lower than the value from [2]. The uncertainty in the EFT( $\not{\mathcal{L}}$ ) value is expected to be  $\gamma |\mathbf{P}| \rho_d^2 \sim 0.4\%$ , and so it is very unlikely that higher order contributions will bring the EFT( $\not{\mathcal{L}}$ ) value into agreement with the value from ref. [2] at this energy. A similar, but much weaker statement can be made about the cross section at  $E = 10$  keV.

A measure of the accuracy of our calculation can be determined by examining the deuteron photo-dissociation cross section, which is related to the capture cross section by

$$\sigma(\gamma d \rightarrow np) = \frac{2M_N(E_\gamma - B)}{3E_\gamma^2} \sigma(np \rightarrow d\gamma) \quad , \quad (19)$$

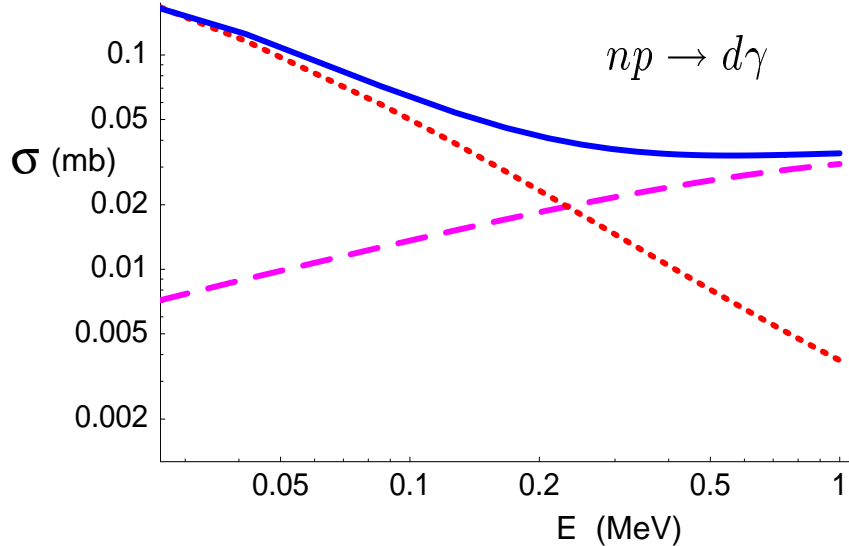


FIG. 1. The cross section for  $np \rightarrow d\gamma$  as a function of the center-of-mass kinetic energy  $E$  in MeV. The dotted curve is the contribution from M1-capture, the dashed curve is the contribution from E1 capture and the solid curve is the sum of the M1 and E1 capture cross sections. Both the vertical and horizontal axes are logarithmically scaled.

| $E$ (MeV)              | $\sigma(np \rightarrow d\gamma)$ |                               |            | ENDF [2]<br>(mb) |
|------------------------|----------------------------------|-------------------------------|------------|------------------|
|                        | M1 (mb)                          | EFT( $\not{\pi}$ )<br>E1 (mb) | M1+E1 (mb) |                  |
| $1.264 \times 10^{-8}$ | 334.2                            | $5.1 \times 10^{-6}$          | 334.2 (*)  | 332.0            |
| $5.0 \times 10^{-4}$   | 1.668                            | $1.0 \times 10^{-3}$          | 1.669(4)   | 1.660            |
| $1.0 \times 10^{-3}$   | 1.171                            | $1.42 \times 10^{-3}$         | 1.173(4)   | 1.193            |
| $5.0 \times 10^{-3}$   | 0.496                            | $3.17 \times 10^{-3}$         | 0.499(4)   | 0.496            |
| $1.0 \times 10^{-2}$   | 0.329                            | $4.48 \times 10^{-3}$         | 0.333(4)   | 0.324            |
| $5.0 \times 10^{-2}$   | 0.0987                           | $9.84 \times 10^{-3}$         | 0.109(3)   | 0.108            |
| 0.100                  | 0.0501                           | 0.0136                        | 0.064(2)   | 0.0633           |
| 0.500                  | 0.00803                          | 0.0260                        | 0.034(1)   | 0.0345           |
| 1.00                   | 0.00375                          | 0.0310                        | 0.035(1)   | 0.0342           |

TABLE I. The cross section for  $np \rightarrow d\gamma$  in millibarns as a function of the nucleon center-of-mass energy,  $E$ . The counterterm  ${}^{\not{\pi}}L_{np}$  is fit to reproduce a cross section of 334.2 mb at an incident neutron speed of  $|\mathbf{v}| = 2200$  m/s. The fact that this cross section is an input is denoted by the asterisk (\*). The numbers in parenthesis are the uncertainty in the last digit, and are estimated by assigning a fractional error of  $(\gamma\rho_d)^4 = 0.028$  to the E1 cross section and a fractional error of  $\gamma|\mathbf{P}|\rho_d^2$  to the M1 cross section. The last column is the total cross section as extracted from the on-line nuclear data center [2].

where  $E_\gamma$  is the incident photon energy and the deuteron is at rest. A comparison between the low-energy cross section computed with EFT( $\not{\pi}$ ) and high precision experimental values can be seen in table II. A detailed and very illuminating discussion of the experiments that contributed to these data points can be found in ref. [10]. In addition, a detailed comparison

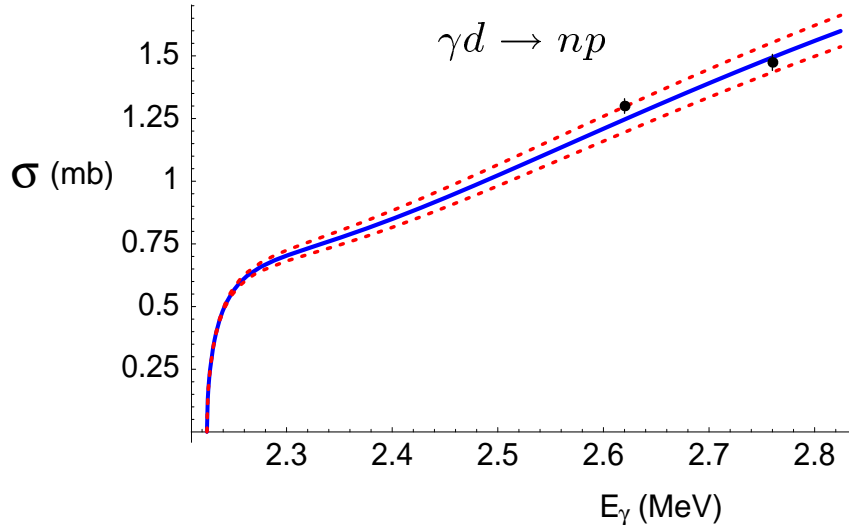


FIG. 2. The cross section for  $\gamma d \rightarrow np$  near threshold, as a function of the incident photon energy in MeV. The solid curve corresponds to the cross section computed in EFT( $\pi$ ). The two dotted curves correspond to the uncertainty in the EFT( $\pi$ ) calculation as estimated by the method described in the text. The two data points with error bars can be found in table II.

| $E_\gamma$ (MeV) | $\sigma(\gamma d \rightarrow np)$ |                         |            | expt. [10]<br>(mb) |
|------------------|-----------------------------------|-------------------------|------------|--------------------|
|                  | M1 (mb)                           | EFT( $\pi$ )<br>E1 (mb) | M1+E1 (mb) |                    |
| 2.62             | 0.380                             | 0.866                   | 1.25(5)    | $1.300 \pm 0.029$  |
| 2.76             | 0.327                             | 1.167                   | 1.50(6)    | $1.474 \pm 0.032$  |
| 4.45             | 0.128                             | 2.353                   | 2.48(9)    | $2.43 \pm 0.17$    |
| 5.97             | 0.084                             | 2.122                   | 2.21(8)    | $2.162 \pm 0.099$  |
| 6.14             | 0.081                             | 2.084                   | 2.17(8)    | $2.190 \pm 0.100$  |
| 7.25             | 0.066                             | 1.838                   | 1.90(7)    | $1.882 \pm 0.011$  |
| 7.39             | 0.065                             | 1.808                   | 1.87(7)    | $1.840 \pm 0.150$  |
| 7.60             | 0.063                             | 1.764                   | 1.83(7)    | $1.803 \pm 0.016$  |
| 7.64             | 0.062                             | 1.756                   | 1.82(7)    | $1.810 \pm 0.028$  |
| 8.14             | 0.058                             | 1.656                   | 1.71(6)    | $1.800 \pm 0.130$  |
| 8.80             | 0.053                             | 1.534                   | 1.59(6)    | $1.586 \pm 0.011$  |
| 9.00             | 0.052                             | 1.500                   | 1.55(6)    | $1.570 \pm 0.036$  |

TABLE II. The cross section for  $\gamma d \rightarrow np$  in millibarns computed in EFT( $\pi$ ) and the experimental values taken from pages 78 and 79 of ref. [10]. The EFT( $\pi$ ) cross section is comprised of the E1 amplitude computed to order N<sup>3</sup>LO and the M1 amplitude computed to NLO. The theoretical uncertainties are estimated in the same way as those in table I.

between the predictions of potential models, in particular the Bonn r-space potential, with these data can also be found in [10]. For the two lowest energy data points the uncertainties in the EFT( $\pi$ ) calculation are seen to be nearly a factor of two larger than the experimental uncertainties at this order. A plot of the break-up cross section in Fig. (2), along with



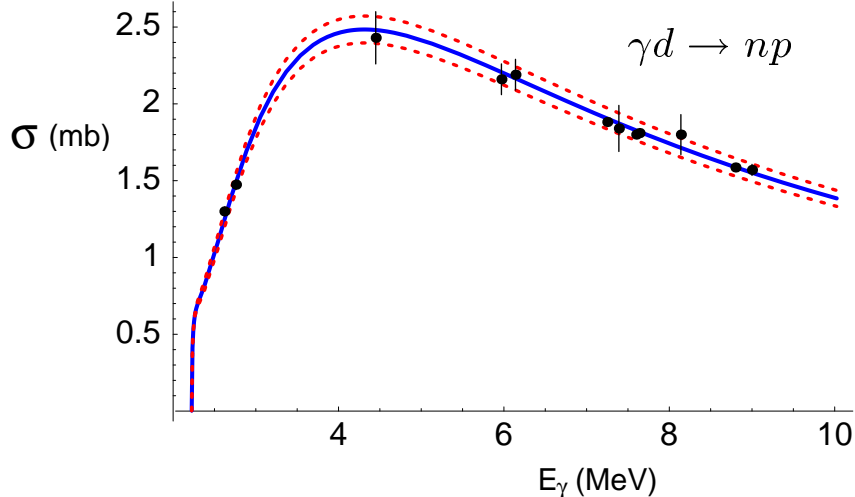


FIG. 3. The cross section for  $\gamma d \rightarrow np$  as a function of the incident photon energy in MeV. The solid curve corresponds to the cross section computed in  $\text{EFT}(\pi)$ . The two dotted curves correspond to the uncertainty in the  $\text{EFT}(\pi)$  calculation as estimated in the text. The data points with error bars can be found in table II.

the two low-energy data points, clearly shows the need for more data in this low-energy region. A few more high precision measurements between  $\sim 2.5$  MeV and  $\sim 4.0$  MeV would provide important constraints on the M1 and E1 amplitudes in the energy region relevant to big-bang nucleosynthesis. It does appear that the  $\sim 3\%$  uncertainty in the E1 cross section that we have estimated to arise from unknown higher order contributions may be an over-estimate. Fig. (3) hints that a  $1\sigma$  error of 1% or 2% might be appropriate, but this cannot be justified from  $\text{EFT}(\pi)$  alone. Given that the  $\text{EFT}(\pi)$  at  $\text{N}^3\text{LO}$  reproduces the E1 amplitude very well, and that there are only two precise data points in the energy region that is sensitive to the M1 amplitude, it is unlikely that pushing the  $\text{EFT}(\pi)$  computation to one higher order would lead to a noticeable difference in cross section. Even at this order in the  $\text{EFT}(\pi)$  expansion, we find good agreement with potential model calculations [10].

Returning to the  $np \rightarrow d\gamma$  capture process, for energies above  $\sim 300$  keV the cross section is dominated by E1 capture and hence the uncertainty in our calculation is essentially the uncertainty in the E1 cross section,  $\sim 3\%$ . In order to further reduce this uncertainty down to  $\sim 1\%$  a  $\text{N}^4\text{LO}$  calculation of the E1 amplitude is required. As we have discussed previously, at  $\text{N}^4\text{LO}$  there is a contribution from a local four-nucleon-one-electric-photon interaction that is not constrained by nucleon-nucleon scattering, but could be determined by the deuteron photo-disintegration cross section. The appearance of such an operator is not restricted to effective field theory as such interactions will also arise in potential model calculations of this amplitude, making roughly the same size contribution. An example of this is the deuteron quadrupole moment [16,17]. To describe the lower energy regime to higher precision, the M1 amplitude will need to be computed to  $\text{N}^2\text{LO}$  or higher. At this order there will be additional counterterms, beyond  ${}^{\#}L_{np}$  that will need to be determined by data. Fig. (2) suggests that the existing two data points in this region may not be sufficient to achieve this.

In conclusion, we have examined the radiative capture process  $np \rightarrow d\gamma$  in the pionless

nucleon-nucleon effective field theory. An analytic expression for the cross section in the energy region relevant to big-bang nucleosynthesis is presented and is expected to reproduce the true cross section at the few percent level. It is simple to relate the rate for  $np \rightarrow d\gamma$  to the cross section for  $\gamma d \rightarrow np$  and our calculation agrees very well with the existing data. There is motivation to perform high precision measurements of the deuteron photodisintegration cross section at very low energies, to tightly constrain the M1 contribution to the cross section.

We would like to thank Gautam Rupak and Scott Burles for useful discussions. We would also like to thank Baha Balantekin, Wick Haxton and Brad Keister for bringing this issue to our attention. This work is supported in part by the U.S. Dept. of Energy under Grants No. DE-FG03-97ER41014.

## REFERENCES

- [1] S. Burles, K. M. Nollet, J. W. Truran and M. S. Turner, *Phys. Rev. Lett.* **82**, 4176 (1999).
- [2] ENDF/B online database at the NNDC Online Data Service, <http://www.nndc.bnl.gov>.
- [3] M. S. Smith, L. H. Kawano and R. A. Malaney, *Astrophys. J. Suppl. Ser.* **85** 219 (1993).
- [4] D.B. Kaplan, M.J. Savage and M.B. Wise, *Phys. Lett. B* **424**, 390 (1998); *Nucl. Phys. B* **534**, 329 (1998).
- [5] D.B. Kaplan, M.J. Savage and M.B. Wise, *Phys. Rev. C* **59**, 617 (1999).
- [6] J. -W. Chen, G. Rupak and M. J. Savage, [nucl-th/9902056](#).
- [7] M. J. Savage, K. A. Scaldeferri, Mark B. Wise, *Nucl. Phys. A* **652**, 273 (1999).
- [8] H. A. Bethe, *Phys. Rev.* **76**, 38 (1949); H. A. Bethe and C. Longmire, *Phys. Rev.* **77**, 647 (1950).
- [9] H. P. Noyes, *Nucl. Phys.* **74**, 508 (1965).
- [10] *Photodisintegration of the Deuteron: A Review of Theory and Experiment*, by H. Arenhovel and M. Sanzone, published by Springer-Verlag, 1991, ISBN 3-211-82276-3.
- [11] J.W. Chen, H. W. Griesshammer, M. J. Savage and R. P. Springer, *Nucl. Phys. A* **644**, 221 (1999); *Nucl. Phys. A* **644**, 245 (1999).
- [12] D. O. Riska and G. E. Brown, *Phys. Lett. B* **38**, 193 (1972).
- [13] J.J. de Swart, C.P.F Terheggen and V.G.J. Stoks, [nucl-th/9509032](#).
- [14] V.G.J. Stoks, R.A.M. Klomp, C.P.F. Terheggen and J.J. de Swart, *Phys. Rev.* **C49** (1994) 2950.
- [15] A.E. Cox, S.A.R. Wynchank and C.H. Collie, *Nucl. Phys.* **74**, 497 (1965).
- [16] B.S. Pudliner, V.R. Pandharipande, J. Carlson, S.C. Pieper and R.B. Wiringa, [nucl-th/9705009](#).
- [17] D. R. Phillips and T. D. Cohen, [nucl-th/9906091](#).